

Deep Learning Descriptor Hybridization with Feature Reduction for Accurate Cervical Cancer Colposcopy Image Classification

Saurabh Saini^a, Kapil Ahuja^{a,**}, Siddhartha Chennareddy^a, Karthik Boddupalli^a

^a*Math of Data Science & Simulation (MODSS) Lab, Computer Science & Engineering, IIT Indore, Indore, 453552, Madhya Pradesh, India*

ABSTRACT

Cervical cancer stands as a predominant cause of female mortality, underscoring the need for regular screenings to enable early diagnosis and preemptive treatment of pre-cancerous conditions. The transformation zone in the cervix, where cellular differentiation occurs, plays a critical role in the detection of abnormalities. Colposcopy has emerged as a pivotal tool in cervical cancer prevention since it provides a meticulous examination of cervical abnormalities. However, challenges in visual evaluation necessitate the development of Computer Aided Diagnosis (CAD) systems. We propose a novel CAD system that combines the strengths of various deep-learning descriptors (ResNet50, ResNet101, and ResNet152) with appropriate feature normalization (min-max) as well as feature reduction technique (LDA). The combination of different descriptors ensures that all the features (low-level like edges and colour, high-level like shape and texture) are captured, feature normalization prevents biased learning, and feature reduction avoids overfitting. We do experiments on the IARC dataset provided by WHO. The dataset is initially segmented and balanced. Our approach achieves exceptional performance in the range of **97%-100%** for both the normal-abnormal and the type classification. A competitive approach for type classification on the same dataset achieved 81% – 91% performance.

© 2024 Elsevier Ltd. All rights reserved.

1. Introduction

Cervical cancer is a serious health concern for women aged 15–44, ranking second in fatality after breast cancer with 340,000 deaths annually Xu et al. [2017]. It is also the second most diagnosed cancer in women, with more than 600,000 annual cases Sung et al. [2021]. The main cause of this is the Human Papilloma Virus (HPV) transmitted through sexual contact Siegel et al. [2021].

Early screening programs can save lives since this cancer is considered incurable in the advanced stages Yusufaly et al. [2020]. Screening methods include visual inspection with acetic acid (VIA), HPV test, pap smear, and colposcopy Aina et al. [2019]. Colposcopy is a widely used method that involves taking pictures of the cervix after applying acetic acid Hua et al. [2020]. This helps identify the various degrees of abnormalities visible in shades of white Mayrand et al. [2007];

Melnikow et al. [2018]; Schneider [2017]. Hence, we focus on this method.

There is a shortage of expert healthcare professionals who can accurately classify cervical colposcopy cancer images (into normal-abnormal and different types). Hence, Computer Aided Diagnosis (CAD) systems are preferred. In this study, we propose one such system.

CAD systems consist of feature extraction, and then image classification. For colposcopy images, texture, shape, edge, and colour are the important features Asiedu et al. [2018]; Yan et al. [2021]. Among the two available feature extraction techniques, i.e., handcrafted descriptors and deep learning descriptors, the latter have been shown to perform better. This is because these deep learning descriptors capture both low-level features (edges and colour) as well as high-level features (texture and shape) well Chandran et al. [2021]; William et al. [2018]. The classification has been typically done using a Support Vector Machine (SVM) Asiedu et al. [2018]; Zhang et al. [2020]. On different datasets, the performance in the range of 81%-96% has been achieved Saini et al. [2020]; Xu et al. [2017]; Wimpy and Suyanto [2019].

**Corresponding author:
e-mail: kahuja@iiti.ac.in (Kapil Ahuja)

In this work, we propose a novel CAD system for colposcopy images that substantially improves the existing systems. The different components of our system are given below.

Descriptors and Classifier:

- We choose three different deep-learning descriptors ResNet50, ResNet101, and ResNet152. This is because ResNet is the best model for removing the vanishing gradient issue, which is commonly encountered in deep-learning models. The individual ResNets do not achieve higher accuracy, and hence, we fuse the descriptors. The fusion of these descriptors is new and has not been applied to colposcopy images.
- Since the features come from different descriptors, normalization of these features is important. This ensures fair treatment of all features and improves the robustness of the machine-learning model. There are various ways of normalization, i.e., z-scored normalization, variable stability scaling, min-max normalization, etc. Singh and Singh [2020]. For us, min-max normalization works well.
- Since we fuse features from different descriptors, there is a risk of overfitting the data, and hence, we apply a feature reduction technique. There are several approaches for reducing features, i.e., Principal Component Analysis (PCA), Independent Component Analysis (ICA), Factor Analysis (FA), Linear Discriminant Analysis (LDA), etc. Jia et al. [2022]; Tawalbeh et al. [2023]; Wahab et al. [2011]. In our case, LDA provides the best results.
- For the classification of colposcopy images, we apply linear SVM, a computationally efficient classification algorithm.

Dataset and Results:

- Our research utilises a standard dataset available from the International Agency for Research on Cancer (IARC), as provided by the World Health Organization (WHO). As far as we know, only one work has been tested on the IARC dataset, against which we compare, i.e., Dash et al. [2023]. The dataset is preprocessed via segmentation and balancing
- For the normal-abnormal classification, we obtain 97% – 99% specificity, sensitivity, and accuracy. No one has done this type of classification on the IARC dataset before. For the type classification (Type 1, Type 2, and Type 3), we obtain 100% specificity, sensitivity, and accuracy. These results are substantially better than 81% – 91% values obtained in Dash et al. [2023].

The rest of this manuscript consists of four more sections. In Section 2, we discuss the past work done in this domain. Our CAD system is described in Section 3. In Section 4, we give results. Finally, conclusion and future work are given in Section 5.

2. Literature Review

The past work done using deep learning for the normal-abnormal and the type classifications for colposcopy images is summarized in Table 1. As evident from this table, column 1 specifies the different methodologies, column 2 describes the kind of classification used, column 3 refers to the dataset, column 4 indicates whether or not data augmentation has been used, and the remaining columns provide classification performance measures.

The first two approaches Saini et al. [2020]; Xu et al. [2017] worked on the National Cancer Institute (NCI) dataset of colposcopy images for the normal-abnormal classification and achieved performances in the range of 81%-88%. The next two approaches Chandran et al. [2021]; Wimpy and Suyanto [2019] tested their work on the Intel dataset for the type classification (and not the normal-abnormal), and achieved performances in the range of 92%-96%. The fifth study Dash et al. [2023], worked on the same dataset as we do, however, this work did only the type classification, and achieved 90.62% specificity, 81.24% sensitivity, 81.24% accuracy.

As evident from previous studies, the performance range has been from 81% to 96%. With our proposed CAD system, we achieve performance in the range of 97% – 100%.

3. Methodology

In this section, we discuss the various components of our proposed CAD system, which includes feature extraction; feature fusion and normalization; feature reduction; and classification. These components are shown in Fig. 1, and discussed in the respective subsections below.

3.1. Feature Extraction

As mentioned earlier, deep-learning models capture both the low-level (edge and colour) and the high-level (shape and texture) features well Amziane et al. [2023]; Buddhavarapu et al. [2020]; Pereira et al. [2024]. In this study, we use three pre-trained deep-learning models of the ResNet family, which are ResNet50, ResNet101, and ResNet152. This is because they address the vanishing gradient problem common in deep neural networks. They achieve this by skipping connections, as shown in Fig. 2. Here, three weighted layers (with ReLU activation function) are skipped.

These models can be used for not just feature extraction with a separate classifier (referred as descriptors), but for end-to-end classification as well. For us, the latter approach did not give promising results, and hence, we use the former. To achieve this, we remove all the fully connected and classification layers from the three models, which returns 2048-length descriptors for each input image.

3.2. Feature Fusion and Normalization

The features of individual feature extraction methods are not sufficient to classify the colposcopy images, and hence, we fuse them together by concatenation Amin et al. [2020]; Khan et al.

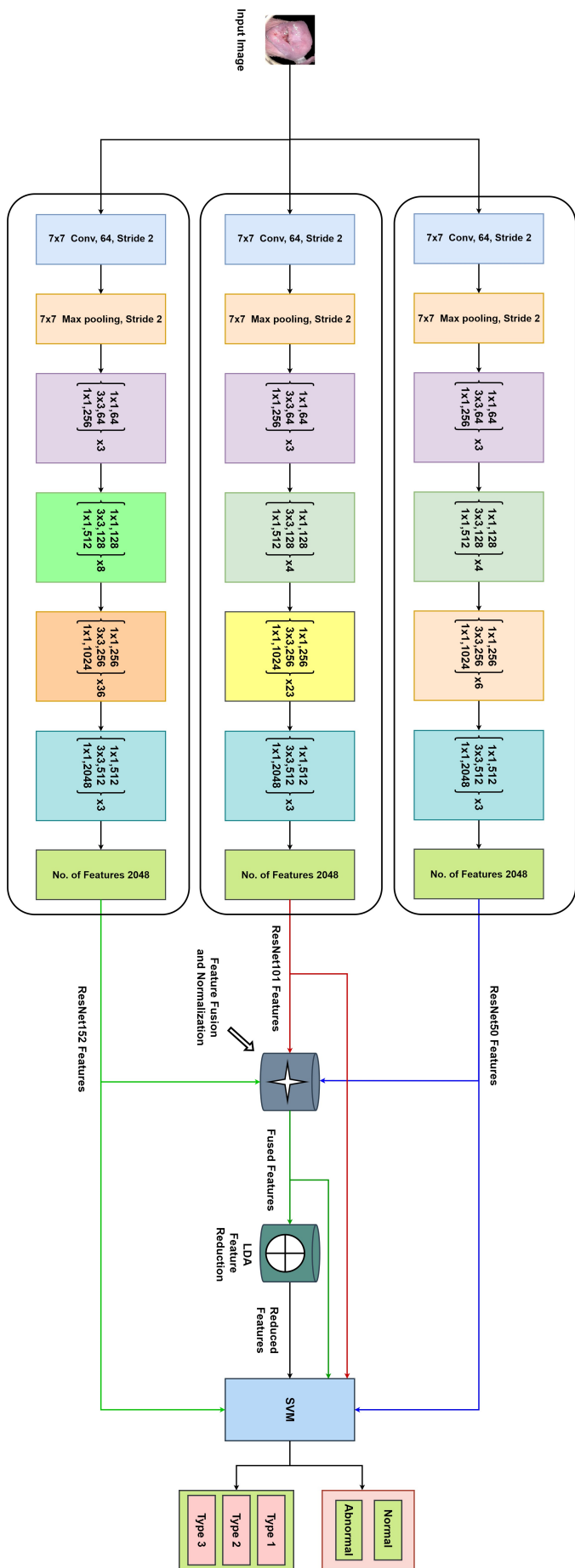
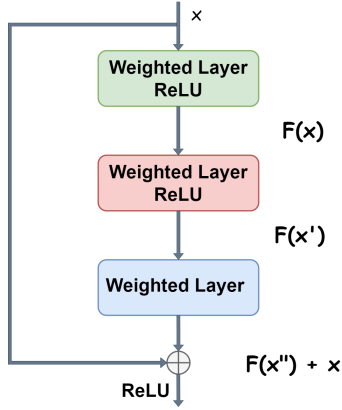


Table 1. Past work in classification of colposcopy images.

Methods	Classification Type	Dataset	Data Augmentation	Sp.(%)	Sen.(%)	Acc.(%)
CaffeNet Xu et al. [2017]	Normal/ Abnormal	US NCI Guanacaste Herrero et al. [1997]	No	83.40	88.30	83.42
ColpoNet Saini et al. [2020]	Normal/ Abnormal	NCI Dataset Saini et al. [2020]	Rotate, Flip, Shift, Scale	–	–	81.35
CapsNet Wimpy and Suyanto [2019]	Type1/ Type2 Type3	Intel ODT Dataset Schwaiger et al. [2012]	No	–	–	94.98
CYENET Chandran et al. [2021]	Type1/ Type2 Type3	Intel ODT Dataset Schwaiger et al. [2012]	Rotate, Crop, Change of Light	96.20	92.40	92.30
Inception- ResNet-V2 Dash et al. [2023]	Type1/ Type2 Type3	IARC Dash et al. [2023]	Rotate, Flip, Change of Light, Contrast	90.62	81.24	81.24

**Fig. 2. Skip connection building block for Resnet50/101/152**

[2020]. Next, we normalize the features to prevent the classification model from bias learning and ensure fair comparisons between different units or measurement scales. There are various ways available to normalize the features, i.e., z-scored normalization, variable stability scaling, min-max normalization, etc. Singh and Singh [2020]. For us, the min-max normalization technique, which scales the features in the range between 0 and 1, works the best. It is formulated as follows:

$$s_{\text{scaled}} = \frac{s - s_{\min}}{s_{\max} - s_{\min}}, \quad (1)$$

where s_{scaled} is the scaled value, s is the original value of the feature, s_{\min} is the minimum value among all the feature values, and s_{\max} is the maximum value, again, among all the feature values.

3.3. Feature Reduction

Since we concatenate the features of different feature extraction methods, this may increase the computational complexity of the subsequent classification and overfit the machine learning model due to the redundant nature of the features. Therefore, a feature reduction method is needed. There are several methods available for feature reduction, such as Principal Component Analysis (PCA), Independent Component Analysis (ICA), and Linear Discriminant Analysis (LDA) Jia et al. [2022]; Tawalbeh

et al. [2023]; Wahab et al. [2011]. LDA is usually very effective for classification tasks due to its ability to maximize the separation between classes Martinez and Kak [2001]. For us too, it works the best.

3.4. Classifier

SVM has emerged as a powerful tool for machine learning and pattern recognition tasks. Their ability to achieve high generalization performance, even with limited training data, has made SVM a preferred choice in various domains. For us, the basic linear SVM works well.

4. Data Preprocessing and Experimental Results

Here, we first describe the data preprocessing and then give our experimentation results.

4.1. Data Preprocessing

We use the publicly available dataset from the International Agency for Research on Cancer (IARC) provided by the World Health Organization (WHO). The original colposcopy images are of 800×600 pixels. We rescale all images to 224×224 to optimize the computational resources. These images not only contain the cervical region (Region Of Interest or ROI), but they also contain some artifacts that are not relevant. Therefore, we segment the images using a method proposed by Dash et al. [2023] to reduce the impact of additional artifacts beyond ROI. Some images are discarded during the segmentation process because the cervix region is not properly visible in the images, and after segmentation, we were left with only an irrelevant region. Fig. 3 shows some sample of original images and their segmented counterparts.

The total number of original images and segmented images for normal-abnormal are given in columns 2 and 3 of Table 2 and for types in columns 2 and 3 of Table 3. As evident from these tables, the data is imbalanced. To address this, we employ various transformations such as contrast, brightness, rotation, and translation Dash et al. [2023]. Specifically, for the normal-abnormal classification, where abnormal images are the majority, we augment the normal images to match the number

of abnormal ones. This results in 374 images of each class, as in column 4 of Table 2, for a total of 748 images, as in column 5 of Table 2.

To balance the types, we follow the methodology outlined in Dash et al. [2023]. Here, we increase the number of images for the class with the fewest samples by a factor of 5 by rotating and flipping. We match the images of the other two classes with the final number obtained above (again by rotating and flipping). This results in 315 images for each class, as given in column 4 of Table 3. To further increase the data, we perform random variations of contrast, brightness, rotation, and translation. This results in 1575 images for each class for a total of 4725 images, as given in columns 5 and 6 of Table 3, respectively.

Table 2. Dataset balancing and diversification for the normal-abnormal classification.

Category	Original Image	Segmented Images	Random Variation (Contrast, Brightness, Rotation, Translation)	No. of Images
Normal	86	75	374	748
Abnormal	483	374	374	

Table 3. Dataset balancing and diversification for the type classification.

Category	Original Image	Segmented Images	Rotation & Flip Operation	Random Variation (Contrast, Brightness, Rotation, Translation)	No. of Images
Type 1	318	226	315	1575	4725
Type 2	106	63	315	1575	
Type 3	147	87	315	1575	

4.2. Experimental Results

To assess the performance of our system, we use standard metrics such as sensitivity, specificity, and accuracy.

Sensitivity measures the ability of the model to identify positive instances out of the total actual positives. It is calculated as follows:

$$Sensitivity = \frac{TP}{TP + FN}, \quad (2)$$

where TP and FN mean True Positive and False Negative, respectively.

Specificity assesses the capability of the model to identify negative instances out of the total actual negatives. It is formulated as follows:

$$Specificity = \frac{TN}{TN + FP}, \quad (3)$$

where TN and FP mean True Negative and False Positive, respectively.

Accuracy represents the overall correctness of the classification model and is calculated as the ratio of correctly predicted instances to the total instances:

$$Accuracy = \frac{TP + TN}{TP + FN + TN + FP}, \quad (4)$$

The results for the normal-abnormal classification are presented in Table 4. Here, the first column lists the type of cross-validation performed, the second column gives the feature extraction technique, and the rest of the columns list the values of the performance metrics. It is apparent from the table that while individual ResNet descriptors exhibit modest performance, a notable improvement is observed upon amalgamating all three ResNet descriptors. However, with LDA, we achieve maximum performance (except for specificity, which is slightly reduced). Fig. 4 depicts the performance bar plot corresponding to Table 4.

Next, the results for the type classification are given in Table 5, which follows the same pattern as normal-abnormal classification. We surpass the performance reported in Dash et al. [2023], achieving 100% metrics. Fig. 5 shows the performance bar plot corresponding to Table 5.

Table 4. Performance of the proposed model with 5-fold and 10-fold cross-validation for the normal-abnormal classification.

Validation Techniques	Features Extraction Techniques	Spec. (%)	Sen. (%)	Acc. (%)
5f cross-validation	ResNet50	96.04	88.27	92.10
	ResNet101	95.80	88.29	91.97
	ResNet152	97.19	86.45	91.70
	ResNet50 + ResNet101 + ResNet152	97.96	92.81	95.32
	ResNet50 + ResNet101 + ResNet152 + LDA	97.59	99.17	98.39
	10f cross-validation	ResNet50	97.37	88.80
ResNet101		95.60	88.10	91.85
ResNet152		97.50	89.63	93.31
ResNet50 + ResNet101 + ResNet152		99.08	93.77	96.25
ResNet50 + ResNet101 + ResNet152 + LDA		97.20	99.21	98.26

Table 5. Performance of the proposed model with 5-fold and 10-fold cross-validation for the type classification.

Validation Techniques	Features Extraction Techniques	Spec. (%)	Sen. (%)	Acc. (%)
5f cross-validation	ResNet50	93.19	88.81	91.72
	ResNet101	93.41	88.93	91.93
	ResNet152	93.59	88.67	91.95
	ResNet50 + ResNet101 + ResNet152	97.65	95.27	98.84
	ResNet50 + ResNet101 + ResNet152 + LDA	100	100	100
	10f cross-validation	ResNet50	93.58	89.05
ResNet101		93.68	89.96	92.46
ResNet152		93.84	89.18	92.29
ResNet50 + ResNet101 + ResNet152 + LDA		97.73	95.87	97.12
ResNet50 + ResNet101 + ResNet152 + LDA		100	100	100

5. Conclusion and Future Work

We present a novel CAD system, which combines features of three deep learning descriptors (ResNet50, ResNet101, and ResNet152) with appropriate normalization (min-max) and feature reduction (LDA). These deep learning descriptors capture all kinds of features while normalization ensures that the combination does not introduce bias, and feature reduction avoids overfitting. The classification is done by a linear SVM. The dataset is preprocessed by segmentation and balancing. We test our system on the publicly available IARC dataset provided by

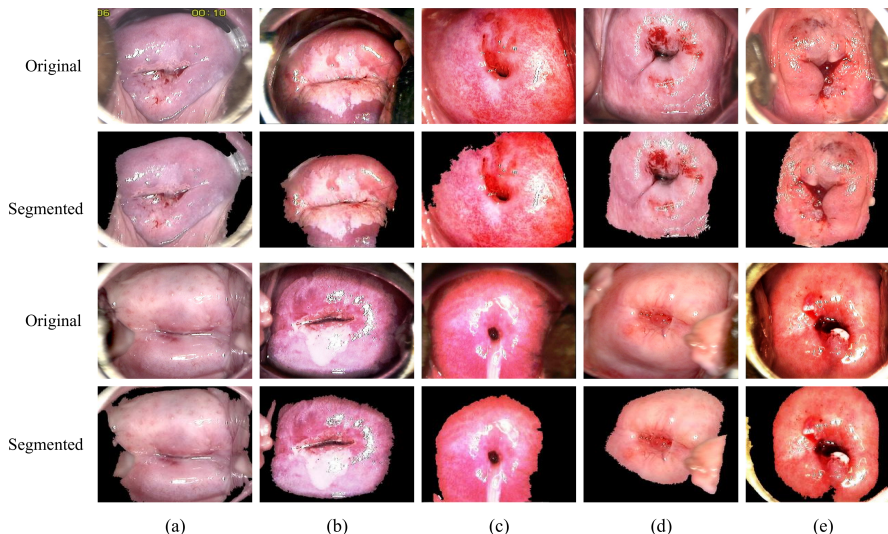


Fig. 3. Rows show the sample of original images and their segmented counterparts. Columns show; (a) Normal (b) Abnormal (c) Type 1 (d) Type 2 (e) Type 3 images.

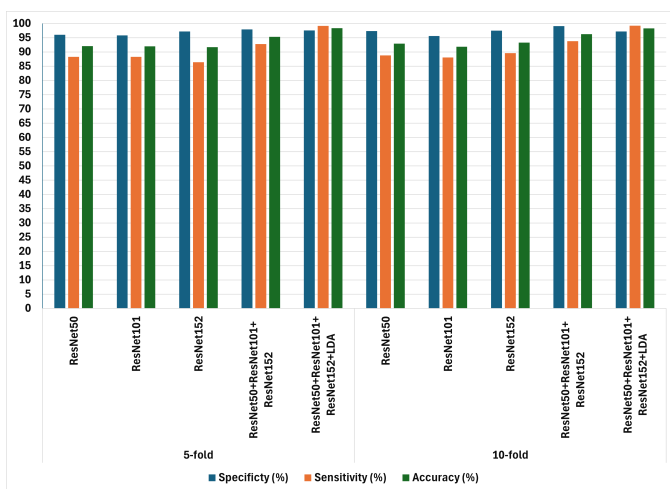


Fig. 4. Performance bar plot for the normal–abnormal classification

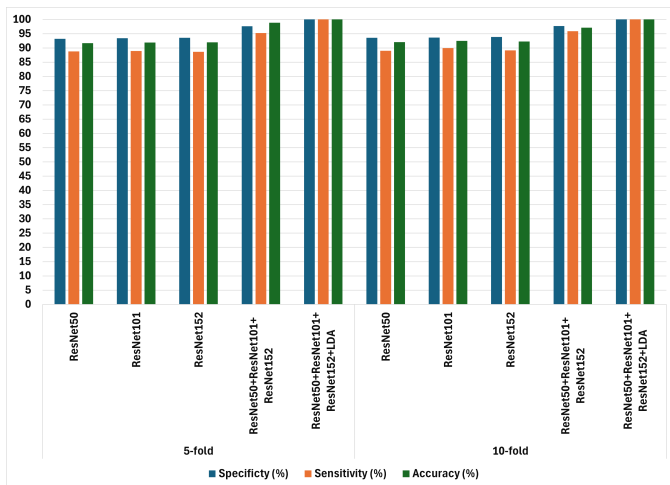


Fig. 5. Performance bar plot for the type classification

the WHO. We achieve above 98% performance for the normal-abnormal and **100%** for the type classification.

One of the future work directions is to test our CAD system on a much larger dataset. WHO has mentioned that they would provide such a dataset soon. A second direction for future work is to study the explainability and interpretability of our CAD system Kim et al. [2005], in turn providing transparency to the decision making. Another future work could be to formulate the combination of different deep neural networks as an optimisation problem as done in different domains Agrawal et al. [2019]; Ahuja et al. [2008]. Finally, it would good to explore the possibility of approximate computing Gupta et al. [2020] in this context.

References

- Agrawal, R., Ahuja, K., Hau Hoo, C., Duy Anh Nguyen, T., Kumar, A., 2019. ParaLarPD: Parallel FPGA router using primal-dual sub-gradient method. *Electronics* 8, 1439.
- Ahuja, K., Watson, L.T., Billups, S.C., 2008. Probability-one homotopy maps for mixed complementarity problems. *Computational Optimization and Applications* 41, 363 – 375.
- Aina, O.E., Adeshina, S.A., Aibinu, A., 2019. Classification of cervix types using convolution neural network (CNN), in: 15th International Conference on Electronics, Computer and Computation, pp. 1–4.
- Amin, J., Sharif, A., Gul, N., Anjum, M.A., Nisar, M.W., Azam, F., Bukhari, S.A.C., 2020. Integrated design of deep features fusion for localization and classification of skin cancer. *Pattern Recognition Letters* 131, 63–70.
- Amziane, A., Losson, O., Mathon, B., Macaire, L., 2023. Msfa-net: A convolutional neural network based on multispectral filter arrays for texture feature extraction. *Pattern Recognition Letters* 168, 93–99.
- Asiedu, M.N., Simhal, A., Chaudhary, U., Mueller, J.L., Lam, C.T., Schmitt, J.W., Venegas, G., Sapiro, G., Ramanujam, N., 2018. Development of algorithms for automated detection of cervical pre-cancers with a low-cost, point-of-care, pocket colposcope. *IEEE Transactions on Biomedical Engineering* 66, 2306–2318.
- Buddharapu, V.G., et al., 2020. An experimental study on classification of thyroid histopathology images using transfer learning. *Pattern Recognition Letters* 140, 1–9.
- Chandran, V., Sumithra, M., Karthick, A., George, T., Deivakani, M., Elakkiya, B., Subramaniam, U., Manoharan, S., et al., 2021. Diagnosis of cervical

- cancer based on ensemble deep learning network using colposcopy images. *BioMed Research International* 2021.
- Dash, S., Sethy, P.K., Behera, S.K., 2023. Cervical transformation zone segmentation and classification based on improved Inception-ResNet-V2 using colposcopy images. *Cancer Informatics* 22, 11769351231161477.
- Gupta, S., Ullah, S., Ahuja, K., Tiwari, A., Kumar, A., 2020. Align: A highly accurate adaptive layerwise Log₂Lead quantization of pretrained neural networks. *IEEE Access* 8, 118899.
- Herrero, R., Schiffman, M.H., Bratti, C., Hildesheim, A., Balmaceda, I., Sherman, M.E., Greenberg, M., Cárdenas, F., Gómez, V., Helgesen, K., et al., 1997. Design and methods of a population-based natural history study of cervical neoplasia in a rural province of Costa Rica: the Guanacaste Project. *Revista Panamericana de Salud Pública* 1, 362–375.
- Hua, W., Xiao, T., Jiang, X., Liu, Z., Wang, M., Zheng, H., Wang, S., 2020. Lymph-vascular space invasion prediction in cervical cancer: exploring radiomics and deep learning multilevel features of tumor and peritumor tissue on multiparametric mri. *Biomedical Signal Processing and Control* 58, 101869.
- Jia, W., Sun, M., Lian, J., Hou, S., 2022. Feature dimensionality reduction: a review. *Complex & Intelligent Systems* 8, 2663–2693.
- Khan, M.A., Rubab, S., Kashif, A., Sharif, M.I., Muhammad, N., Shah, J.H., Zhang, Y.D., Satapathy, S.C., 2020. Lungs cancer classification from ct images: An integrated design of contrast based classical features fusion and selection. *Pattern Recognition Letters* 129, 77–85.
- Kim, S., Murthy, U., Ahuja, K., Vasile, S., Fox, E.A., 2005. Effectiveness of implicit rating data on characterizing users in complex information systems, in: Rauber, A., Christodoulakis, S., Tjoa, A.M.e. (Eds.), *Research and Advanced Technology for Digital Libraries (ECDL 2005)*, Lecture Notes in Computer Science. Springer. volume 3652.
- Martinez, A.M., Kak, A.C., 2001. Pca versus lda. *IEEE Transactions on Pattern Analysis and Machine Intelligence* 23, 228–233.
- Mayrand, M.H., Duarte-Franco, E., Rodrigues, I., Walter, S.D., Hanley, J., Ferenczy, A., Ratnam, S., Coutlée, F., Franco, E.L., 2007. Human papillomavirus dna versus papanicolaou screening tests for cervical cancer. *New England Journal of Medicine* 357, 1579–1588.
- Melnikow, J., Henderson, J.T., Burda, B.U., Senger, C.A., Durbin, S., Soulsby, M.A., 2018. Screening for cervical cancer with high-risk human papillomavirus testing: a systematic evidence review for the us preventive services task force. Agency for Healthcare Research and Quality (US), Rockville (MD).
- Pereira, R., Barros, T., Garrote, L., Lopes, A., Nunes, U.J., 2024. A deep learning-based global and segmentation-based semantic feature fusion approach for indoor scene classification. *Pattern Recognition Letters* 179, 24–30.
- Saini, S.K., Bansal, V., Kaur, R., Juneja, M., 2020. Colponet for automated cervical cancer screening using colposcopy images. *Machine Vision and Applications* 31, 1–15.
- Schneider, V., 2017. Criticism of the pap smear as a diagnostic tool in cervical cancer screening. *Acta Cytologica* 61, 338–344.
- Schwaiger, C., Aruda, M., LaCoursiere, S., Rubin, R., 2012. Current guidelines for cervical cancer screening. *Journal of the American Academy of Nurse Practitioners* 24, 417–424.
- Siegel, R.L., Miller, K.D., Fuchs, H.E., Jemal, A., et al., 2021. Cancer statistics, 2021. *CA: A Cancer Journal for Clinicians* 71, 7–33.
- Singh, D., Singh, B., 2020. Investigating the impact of data normalization on classification performance. *Applied Soft Computing* 97, 105524.
- Sung, H., Ferlay, J., Siegel, R.L., Laversanne, M., Soerjomataram, I., Jemal, A., Bray, F., 2021. Global cancer statistics 2020: GLOBOCAN estimates of incidence and mortality worldwide for 36 cancers in 185 countries. *CA: A Cancer Journal for Clinicians* 71, 209–249.
- Tawalbeh, S., Alquran, H., Alsalatie, M., 2023. Deep feature engineering in colposcopy image recognition: A comparative study. *Bioengineering* 10, 105.
- Wahab, N.I.A., Mohamed, A., Hussain, A., 2011. Fast transient stability assessment of large power system using probabilistic neural network with feature reduction techniques. *Expert systems with applications* 38, 11112–11119.
- William, W., Ware, A., Basaza-Ejiri, A.H., Obungoloch, J., 2018. A review of image analysis and machine learning techniques for automated cervical cancer screening from pap-smear images. *Computer Methods and Programs in Biomedicine* 164, 15–22.
- Wimpy, B., Suyanto, S., 2019. Classification of cervical type image using capsule networks, in: *International Seminar on Research of Information Technology and Intelligent Systems*, IEEE. pp. 34–37.
- Xu, T., Zhang, H., Xin, C., Kim, E., Long, L.R., Xue, Z., Antani, S., Huang, X., 2017. Multi-feature based benchmark for cervical dysplasia classification evaluation. *Pattern recognition* 63, 468–475.
- Yan, L., Li, S., Guo, Y., Ren, P., Song, H., Yang, J., Shen, X., 2021. Multi-state colposcopy image fusion for cervical precancerous lesion diagnosis using BF-CNN. *Biomedical Signal Processing and Control* 68, 102700.
- Yusufaly, T.I., Kallis, K., Simon, A., Mayadev, J., Yashar, C.M., Einck, J.P., Mell, L.K., Brown, D., Scanderbeg, D., Hild, S.J., et al., 2020. A knowledge-based organ dose prediction tool for brachytherapy treatment planning of patients with cervical cancer. *Brachytherapy* 19, 624–634.
- Zhang, T., Luo, Y.m., Li, P., Liu, P.z., Du, Y.z., Sun, P., Dong, B., Xue, H., 2020. Cervical precancerous lesions classification using pre-trained densely connected convolutional networks with colposcopy images. *Biomedical Signal Processing and Control* 55, 101566.